Control synthesis via Impedance-Matching in panchromatic conditions: a generalised framework for moored systems

B. Paduano, E. Pasta, N. Faedo, and G. Mattiazzo

Abstract—**This study focuses on addressing the challenge of integrating the tangled mathematical model of the mooring system into an effective control synthesis. The presented synthesis framework utilises the impedance-matching technique to achieve the desired controller performance by adapting the control parameters to align with the dynamic characteristics of the moored wave energy device. By leveraging this technique, the simulation framework provides a means to effectively incorporate the intricate mooring dynamics into the control synthesis process. Furthermore, this paper aims to delve into the concept of defining a representative control action by examining the input-exciting force of the feedback-controlled system. Through a straightforward case study, the authors demonstrate the significant impact of the mooring on the system dynamics and underscore the applicability of the proposed simulation framework. Moreover, the paper verifies the importance of considering the controlled system's exciting input when addressing control synthesis, particularly in panchromatic conditions.**

Index Terms—**Mooring, wave energy control, impedance-matching, irregular conditions**

I. Introduction

MODELLING a moored wave energy system using a dynamic approach can indeed be time-consuming due to the complex nature of the system [1]. Integrating the mooring system into a wave energy system model for coupled simulations can also pose challenges. However, it is important to consider the impact of the mooring system on the overall dynamics of the system, as it can significantly affect device performance [2], [3]. This is especially true when designing a controller using a model-based approach, as the controller's effectiveness depends on accurate representation of the mooring system dynamics. Therefore, despite the complexities involved, it is essential to include the mooring system in the modelling and analysis of wave energy systems to ensure a comprehensive understanding of their behaviour and performance.

B. Paduano is with Department of Mechanical and Aerospace Engineering, Politecnico di Torino, Turin, 10128 Italy (e-mail: bruno.paduano@polito.it).

E. Pasta is with Department of Mechanical and Aerospace Engineering, Politecnico di Torino, Turin, 10128 Italy (e-mail: edoardo.pasta@polito.it).

N. Faedo is with Department of Mechanical and Aerospace Engineering, Politecnico di Torino, Turin, 10128 Italy (e-mail: nicolas.faedo@polito.it).

G. Mattiazzo is with Department of Mechanical and Aerospace Engineering, Politecnico di Torino, Turin, 10128 Italy (e-mail: giuliana.mattiazzo@polito.it).

Digital Object Identifier:
https://doi.org/10.36688/ewtec-2023-344

Before delving into the analysis, it is important to review the existing literature on the influence of the mooring system on the dynamics and productivity of the device, as well as its incorporation into control synthesis.

The vast majority of analyses in the current wave energy panorama investigate mooring system design for survivability purposes, such as those by Depalo et al. [4], Mao et al. [5], and Wei et al. [6] to name a few.

Cerveira et al. [7] analyses the dynamic response and performance of an arbitrary moored wave energy system, in which the mooring system is described by a nonlinear model. The arbitrary system harvests energy by exploiting surge and heave motion through a proportional controller (where the control force acts as damping on the heave velocity). Although the mooring system's influence on pitch motion was significant, the effect on the harvested energy by device surge and heave motions, which were the PTO controlled degrees of freedom, was minimal. However, the study did not address the design of such a controller.

Fitzgerald and Bergdahl [8] assesses the performance of a generic floating wave energy system under the influence of a set of mooring configurations. The simulations were based on a frequency-domain approach, and the resulting mooring linear model was developed by identifying a linear impedance from catenary analytical equations, and modifying the device dynamics accordingly. The results showed a significant influence of the mooring on device motions, and the identified model was non-representative in conditions significantly different from the linearisation ones.

Gubesch et al. [9] investigates a moored oscillating water column experimentally, comparing a fixed device to the device moored by means of a catenary and a taut solution. The oscillating water column device's performance was significantly affected by the mooring configuration, with a variation of over 50

In Faedo et al. [10], an experimental investigation of a moored pitching wave energy system is conducted. Although the mooring system's influence was outside the scope of the investigation, the control synthesis was achieved by means of a data-based model synthesised from the experimental data, which includes the influence of the station-keeping system.

In [11] and [12], the influence of the mooring system had marginal importance within the study's aim. Furthermore, in these cases, the controller is designed as a proportional actuator, and the associated synthesis was not discussed.

Accordingly, the following key points should be noted:

- The mooring system has a significant effect on the overall dynamics, particularly in pitch and roll motions.
- Dynamic models are needed to capture these significant dynamics, but the computational burden often leads to the use of data-based approaches.
- Despite the importance of the mooring system on device performance, control synthesis is often neglected, and there is a lack of detailed analysis on the performance assessment of moored devices in the current state-of-the-art.

.

With the aim of investigating on the influence of mooring systems in the correlated energy-maximising WEC control synthesis and the associated device performance assessment, within this manuscript, a control-oriented data-based modelling procedure is proposed. By leveraging a data-based modelling it is possible to include the mooring relevant dynamics, and perform a controller synthesis by means of the impedance-matching technique. The target data, used to compute such data-based control-oriented model, is generated by means of a high-fidelity modelling solver, by using a specific set of representative persistently exciting inputs.

Furthermore, when applying impedance-matching theory, the controller is synthesised by matching the optimal controller response to a specific frequency (for detailed information, please refer to Section III). However, it is important to note that the use of impedance-matching theorem-based controllers is not a novel concept in the field, and interested readers are encouraged to refer to [10], [13]–[15] for a comprehensive exploration of this topic.

Moreover, when applying these control strategies in irregular wave conditions, it becomes essential to define a single interpolating frequency in order to compute an effective control action. While choosing a frequency associated with the wave energy spectrum (such as the frequency related to the wave's energetic period, among others) may seem like a reasonable approach, it is crucial to analyse the input exciting spectrum separately, as it can significantly differ from the wave spectrum. Therefore, the selection of the appropriate frequency must be carefully conducted by considering the characteristics of the input exciting spectrum. This step is essential in ensuring an accurate representation of the control action, particularly in irregular sea states where the choice of the interpolating frequency becomes more critical. In order to shed light on this issue, this paper proposes an approach for identifying the appropriate interpolating frequency. By addressing this challenge, we aim to provide valuable insights into the optimisation of the control strategy in a panchromatic environment.

Note that a significant portion of the study presented in this work is based on the findings and insights from [14]. This paper focuses on providing a more extensive and in-depth investigation in the following area:

- Generalisation of the simulation framework for a multi-DoFs moored wave energy system.
- Analysis of the interpolating frequency in irregular sea state conditions.

The reminder of this paper is organised as follows: Section II outlines briefly the numerical models adopted within this study, Section III defines the impedance-matching theory, on which this study is based on. The control synthesis of a general multi-DoF model is depicted in IV, and the inclusion of nonlinear terms, such as the mooring force, is analysed in V and extended in Section VI for panchromatic conditions. Finally, Section VII propose a straightforward application case, and in Section VIII the conclusions are outlined.

II. Numerical modelling

In this study, various numerical models are employed to capture the system dynamics. While a frequency-domain approach can be utilised for purely linear assumptions, it is recognised that a dynamic approach is necessary when modelling a mooring system [16]. Although alternative strategies for computational efficiency, such as those discussed in [17], and the linearisation of nonlinear terms in a spectral-domain fashion [18], can be considered, the following numerical models are employed in this study:

- Device hydrodynamics: the hydrodynamic effects of the device are incorporated using the assumptions outlined in the potential-flow theory [19]. Time-domain simulations are performed by computing the impulse response function based on the well-known Cummins' equation [20].
- Mooring system: the mooring system is modelled using a dynamic lumped-mass model described in [21], and the software adopted is OrcaFlex (OF), being one of the most used in the offshore field [1]. External forces acting on the mooring system are included using the procedure outlined in [14].

III. Impedance-matching-based theory

Within this section, a brief introduction to the control-related mathematical tools, adopted within this study, is provided.

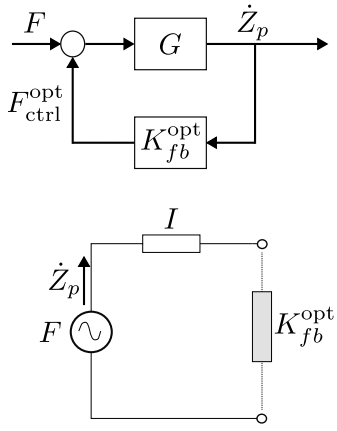

Fig. 1. Impedance-matching principle: equivalent electrical circuit representation.

Figure 1 shows a generic single DoF WEC, feedback controlled by the map $K_{fb}^{opt} : \mathbb{R} \to \mathbb{C}, s \mapsto K_{fb}^{opt}(s)$. The control action $F_{\text{ctrl}}^{\text{opt}}$ can be interpreted as the electric load, which has to be designed, to maximise power extraction from the source, which is represented by the generic force F. Note that $\dot{Z}_p$ represents the velocity of a generic motion of a floating object, and the map $G : \mathbb{R} \to \mathbb{C}, s \mapsto G(s)$ can be easily linked to the hydrodynamic properties of the body.

The resolution of this problem, under its electrical representation can be addressed by means of the so-called impedance-matching theorem [22]. It states that, in order to maximise the power transfer, the load impedance K_{fb}^{opt} needs to be designed as the complex conjugate of the system impedance, which means, in the WEC case:

$$K_{fb}^{\text{opt}} = I^* = G^{-*}. \tag{1}$$

The equation of motion becomes:

$$\begin{aligned} \dot{Z}_p &= G(F - F_{\text{ctrl}}^{\text{opt}}), \\ F_{\text{ctrl}}^{\text{opt}} &= G^{-*}\dot{Z}_p, \end{aligned} \tag{2}$$

in which $F_{\text{ctrl}}^{\text{opt}} : \mathbb{R} \to \mathbb{C}, \omega \mapsto F_{\text{ctrl}}^{\text{opt}}$ is the optimal control action. Although by synthesising the controller in terms of the impedance-matching theorem, the resulting associated optimal control action results to be stable, it is *anti-causal*, since it requires future knowledge of the excitation force, being the response $\dot{Z}_p$ in instantaneous phase with the force $F(\omega)$.

It can be appreciated by the associated closed-loop, *i.e.*:

$$W^{\text{opt}} = \frac{GG^*}{G + G^*}, \tag{3}$$

in which $W^{\text{opt}} : \mathbb{R} \to \mathbb{R}^+, s \mapsto W^{\text{opt}}(\omega)$ is, in essence, an ideal, zero-phase filter. The velocity $\dot{Z}_p$, subject to the optimal control law, is in instantaneous phase with the input force and, moreover, represents a scaled version of same input force.

IV. Control synthesis procedure

Being a wave energy system represented as a multi-DoF with multiple control inputs wave energy system, $G : \mathbb{R} \to \mathbb{C}^{n_{\text{DoF}} \times n_{\text{DoF}}}$, the control force can be defined as $F_{\text{ctrl}} : \mathbb{R} \to \mathbb{C}^{n_c}, \omega \mapsto F_{\text{ctrl}}(\omega)$ represents the controlled actions, being $n_c \subset [1, \ldots, n_{\text{DoF}}]$ the number of the controlled DoFs. Please note that, the application of the impedance-matching theorem in a generic multi-DoFs system is exhaustively described in [15].

To achieve the control synthesis the controlled equivalent system needs to be isolated from the total map. By collecting the first n_c rows of the system G, it is possible to define:

$$G = \begin{bmatrix} G_c & G_{\tilde{c}} \\ G_{0,1} & G_{0,2} \end{bmatrix}, \tag{4}$$

in which $G_c : \mathbb{R} \to \mathbb{C}^{n_c \times n_c}$, and $G_{\tilde{c}} : \mathbb{R} \to \mathbb{C}^{n_{\text{DoF}} - n_c \times n_c}$. Moreover, the external force acting on the system closed-loop can be divided into:

$$F = \begin{bmatrix} F_c \\ F_{\tilde{c}} \end{bmatrix}. \tag{5}$$

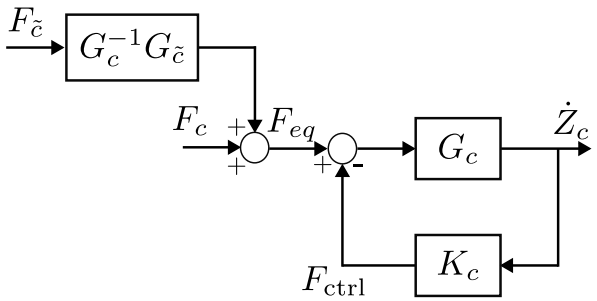

Fig. 2. Generalised application of the impedance-matching principle.

Accordingly, the system response can be described as the I/O system in Figure 2 in which the system G_c is feedback controller by the map K_c, and $\dot{Z}_c \in \mathbb{C}^{n_c}$ are the velocity of the controlled DoFs. Finally, the external force can be figured as an equivalent exciting input F_{eq}, *i.e.*:

$$\begin{aligned} Z_c &= \begin{bmatrix} G_c & G_{\tilde{c}} \end{bmatrix} \begin{bmatrix} F_c \\ F_{\tilde{c}} \end{bmatrix} = G_c F_{eq}, \\ F_{eq} &= F_c + G_c^{-1} G_{\tilde{c}} F_{\tilde{c}}, \end{aligned} \tag{6}$$

Accordingly, it is possible to apply the impedance-matching theory and evaluate the system-associated controller as:

$$\begin{aligned} K_c^{\text{opt}} &= G_c^{-*}, \\ K_c(\omega_m) &= K_c^{\text{opt}}(\omega_m), \end{aligned} \tag{7}$$

where G_c^* represents the para-hermitian complex-conjugate of G_c.

V. Data-based modelling

Within this section, the focus shifts to the definition of the map G_c, which represents the system from the controller's point of view. To ensure the broad applicability of the proposed procedure, it addresses the multi-degree-of-freedom problem with multiple control actions. This allows for a comprehensive investigation of the system's behaviour and control strategies in a wide range of scenarios.

From a general perspective, a system can be characterised by means of several nonlinearities or, moreover, during an experimental investigations (see for example [10]), the computation of a control action based on numerical models can provide unreliable results, since prototyping leads to several uncertainties [23].

Following the impedance-matching approach presented in Section III, the procedure for the identification of a representative device frequency-response, non-parametric, map, so as to effectively leveraging the result in (1), is outlined below.

By leveraging linear assumptions, a multi-DoF wave energy system can be defined, as exposed in Figure 3, by means of the linear map $G_c : \mathbb{R} \to \mathbb{C}^{n_c \times n_c}, \omega \mapsto G_c(\omega)$.

Please note that, the map G_c represents the linear approximation of the system "seen" by the controller map K_c.

The identification of the frequency response $G_c(\omega)$ is achieved by evaluating the associated empirical transfer function estimate, imposing a set of known

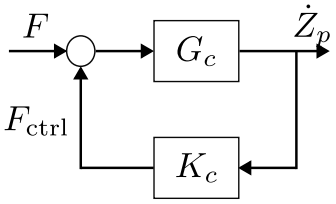

Fig. 3. Schematic representation of a wave energy system under LTI assumption.

(sufficiently exciting) input signals as control exciting forces (*i.e.* $\hat{F}_{\text{ctrl}}$ in Figure 4).

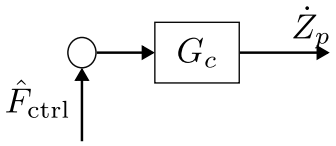

Fig. 4. System frequency response identification.

Although several signals can be employed for the identification of the corresponding frequency responses (see, for instance, [24]), a multisine signal is adopted within this manuscript, taking advantage of *e.g.* its periodicity and bounded spectrum [25]. In

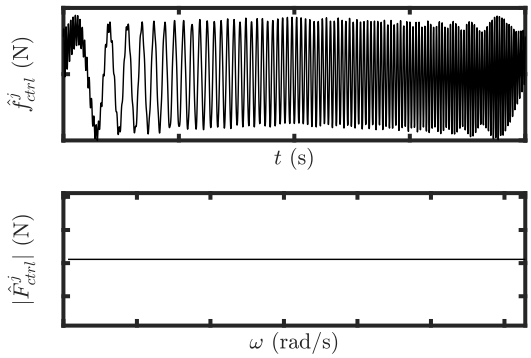

Fig. 5. Multisine signal of the control force: time and frequency domain representation.

particular, the set of multisine signals is built by applying the so-called *Schroeder* phases [26] (an example of a multisine signal is exposed in Figure 5), *i.e.* the representative excitation signal becomes:

$$\begin{aligned}
\hat{f}^j_{\text{ctrl}}(t) &= \begin{bmatrix} 0 & \dots & \hat{f}^j_{\text{ctrl},l}(t) & \dots & 0 \end{bmatrix}^\intercal, \quad \forall l \in [1,\dots,n_c],\\
\hat{f}^j_{\text{ctrl},l}(t) &= \sum_{k=1}^{N_k} a_{j,l}\cos(\omega_k t + \phi_k),\\
\phi_k &= \frac{-k(k+1)}{N_k}, \qquad \forall k \in \{1,\dots,N_k\},
\end{aligned} \tag{8}$$

where $a_{j,l} \in \mathscr{A} \subset \mathbb{R}^+$, $j \in \{1,\dots,N_j\}$, defines the final signal amplitude for the l-th exciting force, with $l \in [1,\dots,n_c]$.

Remark 1. *Please note that, exciting signal $\hat{f}^j_{ctrl,l}$ needs to be designed according to the system response, i.e.:*

- *The frequency bandwidth is chosen in order to excite any relevant dynamics.*
- *The signal (experiment) duration needs to be tuned accordingly, since it naturally relates, in periodic signals, to the frequency discretisation (i.e. the frequency discretisation needs to be small enough to characterise any relevant dynamic).*
- *The associated signal amplitudes are defined accordingly to the operating conditions. For example, in [7], the exciting signal is chosen to have the same energy as the wave frequency motion.*

For further information, the reader is referred to e.g. [27].

Since the model to characterise in terms of a representative linear mapping G_c has, a nonlinear behaviour, the input signal $\hat{f}_{\text{ctrl}}$ needs to be tested under several amplitude conditions $a_{j,l} \in \mathscr{A}$ (see Remark 1). Using each input element in the set $\mathscr{A}$, and corresponding output $\dot{Z}^j_p$, it is possible to construct the average empirical transfer function estimate as

$$G_{c,b,l}(\omega) = \sum_{j=1}^{N_j} \frac{1}{N_j} \frac{\hat{F}^j_{\text{ctrl},l}(\omega)}{\dot{Z}^j_{p,b}(\omega)}, \tag{9}$$

in which $G_{c,b,l} : \mathbb{R} \to \mathbb{C}, \omega \mapsto G_{c,b,l}(\omega)$ constitutes an element of the total map G_c, with $b \in [1,\dots,n_c]$.

VI. On the matching frequency in panchromatic conditions

If the system is excited by means of monochromatic signals (*i.e.* the WEC experiences regular wave conditions), the definition of the matching-frequency (ω_m) is straightforward. Moreover, the application of the proposed phase-matching controller is clearly limiting therefore, the definition of the proper interpolation is discussed herein.

Irregular sea state conditions are defined by means of a wave spectrum, which defines, for any frequency, the probability of a monochromatic exciting component. Although the definition of the matching frequency (*i.e.* ω_m in (7)) can be achieved, in first attempt, by leveraging the characterising frequencies of the wave spectrum (*e.g.* mean, peak, or energy frequency, among others), it needs to be achieved taking into account the equivalent force F_{eq} acting on the controlled system.

Remark 2. *Although in most applications the definition of the map $G_{\eta 2 f_{eq}}$ is straightforward (e.g. if the F_{eq} is equal to the wave first order exciting force, see Section VII-D), in general it can be defined by means of the same procedure exposed in Section V (i.e. by leveraging a data-based model), by defining, as exciting input, a properly-tuned wave profile.*

Therefore, by defining a the $G_{\eta 2 f_{eq}} : \mathbb{R} \to \mathbb{C}^{n_c}, \omega \mapsto G_{\eta 2 f_{eq}}(\omega)$ the map which links the wave elevation to the exciting force F_{eq} (see Remark 2), it is possible to define the associated spectra $S_{f_i} : \mathbb{R} \to \mathbb{R}^{n_c}, \omega \mapsto S_{f_i}(\omega)$, with $i = [1,\dots,n_c]$ as:

$$S_{f_i} = \left(G_{\eta 2 f_{eq_i}}\right)\left(G^*_{\eta 2 f_{eq_i}}\right) S_\eta. \tag{10}$$

Even after the definition of the exciting spectra, the associate matching-frequency still results not univocally defined. In a general perspective, the matching

frequency can be achieved by solving an optimisation, energy-maximising, problem, by leveraging linear data-based models, *i.e.*:

$$\Gamma(\omega_m): \begin{cases} \max\limits_{\omega_m \in \mathbb{R}^+} m_{0,p}, \\ \text{subject to:} \\ m_{0,p} = \sum\limits_{i=1}^{n_c} \int_{\mathbb{R}^+} S_{p_i}(\omega_m)\mathrm{d}\omega, \\ S_{p_i}(\omega_m) = S_\eta(G_{3_i}(\omega_m))(G_{3_i}(\omega_m))^*, \\ G_{3_i}(\omega_m) = G_{1_i}(\omega_m)G_{2_i}(\omega_m), \\ G_1(\omega_m) = W(\omega_m)G_{\eta 2 f_{eq}}, \\ G_2(\omega_m) = K_c(\omega_m)W(\omega_m)G_{\eta 2 f_{eq}}, \\ W(\omega_m) = (G_c(\omega_m)K_c(\omega_m) + \mathbb{I}^{n_c})^{-1}G_c, \\ K_c(\omega_m) = G_c^{-*}(\omega_m), \end{cases}$$

in which, $S_{p_i} : \mathbb{R} \to \mathbb{R}^+, \omega \mapsto S_{p_i}(\omega)$ is the power spectrum of the i-th controlled DoF, $W : \mathbb{R} \to \mathbb{C}^{n_c \times n_c}, \omega \mapsto W(\omega)$ represents the controlled closed loop, $m_{0,p} \in \mathbb{R}^+$ is the sum of the 0-order moment of the corresponding power spectrum S_{p_i}. Moreover, the following frequency responses are defined to assist the current dissertation:

- $G_1 : \mathbb{R} \to \mathbb{C}^{n_c}, \omega \mapsto G_1(\omega)$: is the map between the wave elevation and the controlled DoFs velocity, defined in (VI) according to (10).
- $G_2 : \mathbb{R} \to \mathbb{C}^{n_c}, \omega \mapsto G_1(\omega)$: is the map between the wave elevation and the control actions, defined in (VI).
- $G_3 : \mathbb{R} \to \mathbb{C}^{n_c}, \omega \mapsto G_1(\omega)$: is the map between the wave elevation and the associated power, defined in (VI).

Clearly, within ordinary application cases, the problem is significantly less intricate than the one proposed above (as example see Section VII-D). Therefore, investigating a case-of-study within a single controlled DoF, or if the controlled DoFs are *uncoupled* each other (*i.e.* the matrix G_c is diagonal), it is possible to define a good approximation of the best matching frequency as follows:

- From the spectrum of the exciting force, the associated probability density function can be defined, *i.e.*:
$$\mathcal{P}(S_f) = \frac{S_f}{\int_{\mathbb{R}^+} S_f \mathrm{d}\omega}. \tag{11}$$
- Accordingly, the matching frequency can be defined as the median of the probability density function, *i.e.* the frequency ω_m such that:
$$\int_0^{\omega_m} \mathcal{P}(S_f)\mathrm{d}\omega = \frac{1}{2}. \tag{12}$$

VII. An intuitive application case

Within this section the whole procedure is applied and described in a simple case-of-study. Clearly, the solver under investigation is OF, since it is one of the most used solver in offshore field [1]. A heaving point absorber is investigated. Precisely, the harvested energy can be derived in a certain time interval Δt as:

$$L = \frac{1}{t_2 - t_1} \int_{t_1}^{t_2} \dot{z}_3(\dot{z}_3 k_p + z_3 k_i)\mathrm{d}t. \tag{13}$$

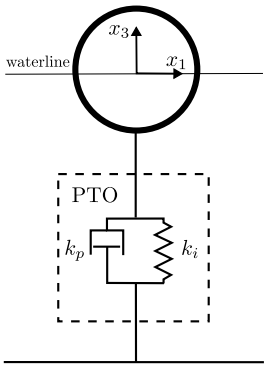

Fig. 6. Schematic representation of the point absorber.

Hence, the controller leverages of a PI structure, and the associated action acts on the x_3 axis of the floating object (see Figure 6). Moreover, by taking advantage of the OF graphic interface, the complete moored system is represented in Figure 7, and the associated properties are reported in Table I.

A. Layout and properties

The point absorber is a spheric floating unit with the CoG located in the geometric centre and, according to its free floating condition, on the waterline. The mooring system is formed by a symmetrical pattern of four semi-taut mooring lines. The bottom catenary section, together with the subsurface buoy, is used to prevent the synthetic section damage by avoiding the clash of the latter with the seabed, and the top one avoids the synthetic line to work in the splash zone, which can be deleterious for a synthetic-made line. The main properties of the system are outlined in Table I.

TABLE I
Moored point absorber properties.

property	symbol	value
Device		
sphere radius (m)	-	4
mass (kg)	$m_{3,3}$	136000
hydrostatic stiffness (N/m)	$h_{k,3,3}$	504000
water depth (m)	w_d	40
Mooring		
anchor radius (m)	ρ_a	60
mooring angle (rad)	β_m	$\frac{\pi}{3}$
catenary s. length (m)	-	10
polyester s. length (m)	-	45
buoy NB (kg)	-	1000

Moreover, since OF is not able to solve the diffraction problem and compute the hydrodynamic parameters, the solver used as BEM is OrcaWave (OW). Given that OW is not able to mesh a generic file, the Nemoh axisymmetric mesher is used. The hydrodynamic parameters are computed and, Figure 8 describes the force-to-velocity response of the point absorber, the map can be written as:

$$\begin{aligned} \dot{Z}_3 &= \jmath\omega G_{d,3,3} F_{\text{eq},3}, \\ F_{\text{eq},3} &= F_{\text{tot},3} + \sum_{i=1, i\neq 3}^{6} \frac{G_{d,3,i}}{G_{d,3,3}} F_{\text{tot,i}}, \end{aligned} \tag{14}$$

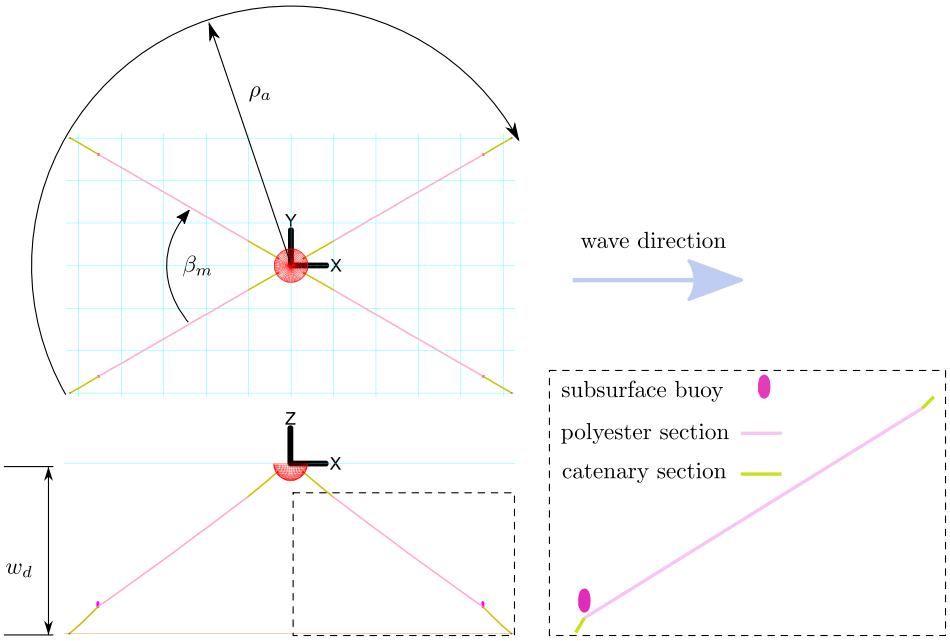

Fig. 7. OF representation of the point absorber. Global axes expressed according to the OF global FoR.

in which, the force-to-velocity map is expressed as $\frac{\hat{Z}_3}{F_{\text{eq},3}} : \mathbb{R} \to \mathbb{C}, \omega \mapsto \frac{\hat{Z}_3}{F_{\text{eq},3}}(\omega)$.

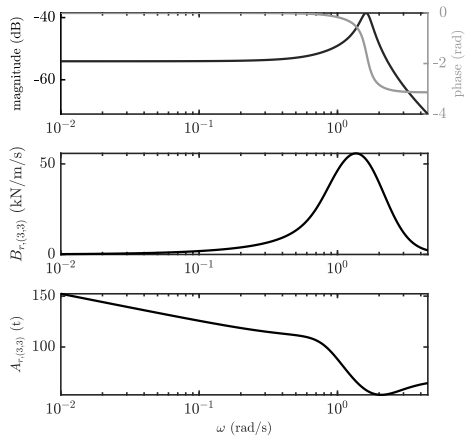

Fig. 8. Point absorber hydrodynamic force-to-position response.

B. Data-based modelling

According to the process described within this chapter, the system needs to be excited on the heave motion by a multisine signal. Starting the analysis on a wave scatter it is possible to define a range of frequency and amplitude. Since the excited motion is the heave one, it is possible, according to a wave spectrum to evaluate the associated spectrum of the excitation force on heave motion by writing:

$$\begin{aligned} S_{F_{eq,3}}(\omega) &= \left|G_{F_{eq,3}}(\omega)\right|^2 S_\eta(\omega), \\ G_{F_{eq,3}}(\omega) &= \frac{F_{eq,3}(\omega)}{\tilde{\eta}(\omega)}, \end{aligned} \tag{15}$$

being $S_\eta(\omega)$ the wave spectrum, and $G_{F_{eq,3}} : \mathbb{R} \to \mathbb{C}, \omega \mapsto G_{F_{eq,3}}(\omega)$ the map between the wave elevation and the equivalent force on heave motion.

By characterising the equivalent force spectrum $S_{F_{eq,3}}(\omega)$, it is possible define a range of frequency and associated amplitude, the moment of the signal $m_{0,F_{eq,(3)}} \in \mathbb{R}^+$ can be described as:

$$m_{0,F_{eq,(3)}} = \int_{\mathbb{R}^+} S_{F_{eq,3}}(\omega)\mathrm{d}\omega. \tag{16}$$

The wave conditions are then presented in Table II and used to construct a representative set of exciting signals.

TABLE II
MOST FREQUENT AND ENERGETIC WAVES OFF THE COAST OF PANTELLERIA

T_e (s)	H_s (m)
3.5	0.375
6.5	1.875

Based on the waves listed[1] in Table II, a series of multisines is generated to represent the system's excitation conditions. Each multisine is designed to have an energy content between that of the most frequently occurring wave and the most energetic one, as described in equation (16). The resulting multisines are illustrated in Figure 9.

By applying the associated control force on the heave axis, it is possible to evaluate the empirical transfer function estimate, as presented in equation (15). The resulting averaged response is depicted in Figure 10 and compared to the BEM-based response.

The dual effect of the mooring system can be observed in the system's response. With the mooring, the resonance frequency shifts to a higher period, indicating a higher stiffness compared to the unmoored system. Additionally, the amplitude of resonance decreases due to the damping effect of the mooring lines.

To assess the control synthesis procedure, the system needs to be tested under monochromatic conditions,

[1]Please note that the chosen waves represent the most occurrent and the most energetic wave condition of the Pantelleria site, in the southern Italy.

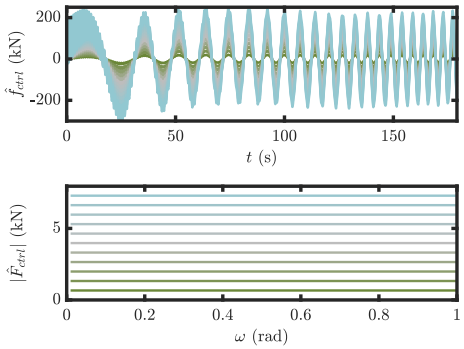

Fig. 9. Exciting inputs.

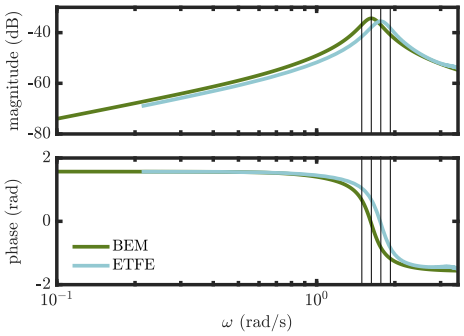

Fig. 10. System I/O force-to-velocity response. The BEM model (hydrodynamics only) is compared with the empirical transfer function estimate evaluated by means of OF. The black lines represent the chosen interpolating frequencies.

where the associated controller is designed. Since the frequency responses are similar outside the resonance region, the influence of the mooring on the control synthesis procedure is examined specifically within the resonance region (refer to Figure 10).

C. Control synthesis procedure

The system can be described in an algebraic block fashion as expressed in Figure 2, in which the controller is figured as the map $K_c : \mathbb{R} \to \mathbb{C}, \omega \mapsto K_c(\omega)$.

Hence, the controller can be synthesised by means of the impedance-matching technique by interpolating the optimal response with a defined controller structure, *i.e.*[2]:

$$\begin{aligned} \dot{Z}_3 &= \jmath\omega G_{d,3,3} F_{\text{eq},3}, \\ K_c^{\text{opt}}(\omega) &= (\jmath\omega G_{d,3,3}(\omega))^{-*}, \\ K_c(\omega) &= k_p + \frac{k_i}{\jmath\omega}, \\ K_c(\omega_m) &= K_c^{\text{opt}}(\omega_m), \quad \omega_m \in [1.49, 1.62, 1.75, 1.88], \end{aligned} \tag{17}$$

Figure 11 displays the optimal closed-loop response of both the moored and unmoored (BEM) systems, as well as the PI-controlled closed-loop response obtained by interpolating the controller to the frequency $\omega_4 = 1.88, \text{rad/s}$. Please note that, an alternative approach to include the adopt an equivalent PI structure is proposed in [28].

[2]Please note that, in the case under investigation for the unmoored device the map $G_c = \jmath\omega G_{d,3,3}$.

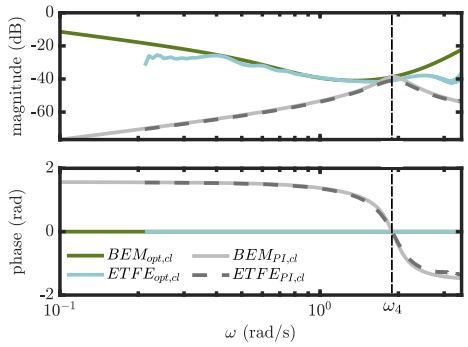

Fig. 11. System closed-loop response.

To assess the effectiveness of the control synthesis, it is necessary to evaluate and compare the power output under regular operating conditions. Therefore, the controllers synthesised with and without the mooring system are incorporated into the moored model. The

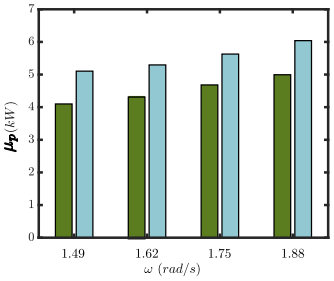

Fig. 12. Average power values of the moored system with the controller synthesised by means of the moored frequency response (cyan bars), and the unmoored one (green bars).

regular sea states are chosen according to the regular frequencies defined above, and the performance are evaluated by means of the average mechanical power, *i.e.*:

$$\begin{aligned} p(t) &= \dot{z}_3(t)(\dot{z}_3(t)k_p + z_3(t)k_i), \\ \mu_p &= \frac{1}{N}\sum_{ii=1}^{N} p_{ii}. \end{aligned} \tag{18}$$

The results are displayed in Figure 12. The analysis shows a significant improvement in the system's performance when the mooring system is included in the control synthesis. On average, there is a 20% increase in power output compared to the case without the mooring system. This highlights the effectiveness of incorporating the mooring system into the control strategy, leading to enhanced power generation capabilities.

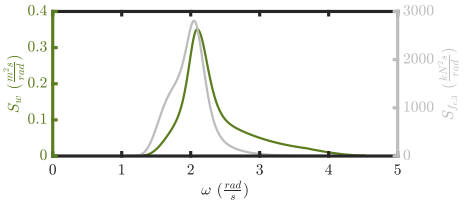

Fig. 13. Wave JONSWAP spectrum in green, and the associated heave excitation force in grey.

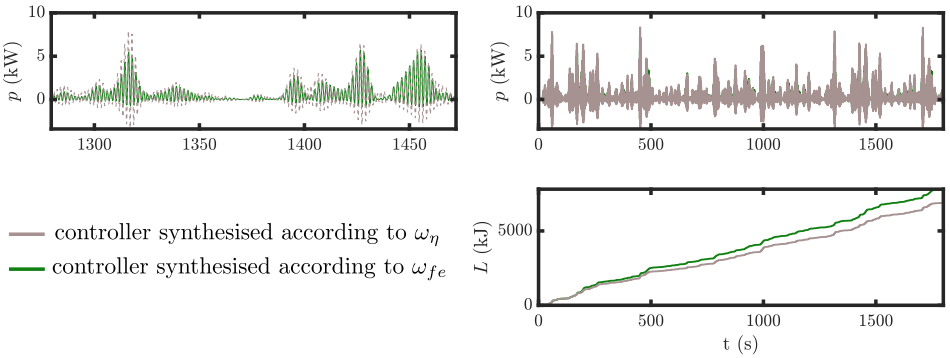

Fig. 14. On the right-hand side of the picture, instantaneous mechanical power and the associated harvested energy. On the left-hand side a zoom on the mechanical power.

D. Towards irregular sea state

So far, the effective influence of the mooring system on the device dynamics and the associated control synthesis has been proved in monochromatic conditions. Within this section, we continue with the proposed approach by utilising a panchromatic exciting input. The system is stimulated by simulating an irregular ocean wave using a JONSWAP spectrum [29]. Accordingly, the excitation force spectrum associated with the irregular ocean wave can be represented as follows:

$$S_{f_e} = S_\eta \left(G_{F_{e,3}} G^*_{F_{e,3}} \right), \tag{19}$$

in which $G_{F_{e,3}} : \mathbb{R} \to \mathbb{C}, \omega \mapsto G_{F_{e,3}}(\omega)$ represents the map between the wave elevation and the heave excitation force, and $\{S_{f_e}, S_\eta\} : \mathbb{R} \to \mathbb{R}, \omega \mapsto \{S_{f_e}(\omega), S_\eta(\omega)\}$ are the heave-associated force spectrum, and the wave one. Both JONSWAP and excitation force spectra are represented in Figure 13.

In the proposed case study, the relationship between the velocity and the associated excitation force is given by the expression:

$$S_{\dot{z}_3} = S_{f_e} \left(\frac{G_{\dot{z}_3} G^*_{\dot{z}_3}}{(G_{\dot{z}_3} K_c + 1)(G_{\dot{z}_3} K_c + 1)^*} \right), \tag{20}$$

in which, $G_{\dot{z}_3} : \mathbb{R} \to \mathbb{C}, \omega \mapsto G_{\dot{z}_3}(\omega)$ is the empirical transfer function estimate of the map between the excitation force and the system heaving velocity. According to the most occurrent wave (see Table II), the control parameters are evaluated by computing the median of the wave and exciting force spectrum. In details, the matching frequencies for both wave and force spectra can be evaluated as:

$$\begin{aligned} \int_0^{\omega_{f_e}} \mathcal{P}(S_{f_e}) \mathrm{d}\omega = \frac{1}{2} \to \omega_{f_e} = 1.74 \text{ rad/s}, \\ \int_0^{\omega_\eta} \mathcal{P}(S_\eta) \mathrm{d}\omega = \frac{1}{2} \to \omega_\eta = 1.66 \text{ rad/s}, \end{aligned} \tag{21}$$

where $\omega_\eta, \omega_{f_e} \subset \mathbb{R}^+$ represent the matching frequencies based on the wave and force spectra, respectively.

In Figure 12, the simulation results are presented, showcasing the outcomes under the specified sea state conditions. It is noteworthy that when the controller is synthesised by interpolating the optimal controller response and defining the frequency based on the excitation force spectrum, a notable increase in harvested energy of up to 13% is observed during the 1800-second simulation.

Additionally, it is intriguing to analyse that synthesising the controller according to the input-exciting (force) spectrum yields a significantly more effective control action. This is evident as the power component dominates, resulting in a reduction of the reactive part minimising the force applied and the maximising power..

VIII. Conclusions

Mooring modelling poses a considerable challenge when attempting to create a representative model that accurately assesses the performance of wave energy systems. The interaction between the device, the waves, and the mooring system adds complexity to the system dynamics and requires careful consideration.

In this study, a comprehensive approach is proposed to address the inclusion of the mooring system's influence in the overall system dynamics and enable effective control synthesis. The key principle used is impedance matching, which ensures that the control action is designed to match the characteristics of the system and optimise its performance. This approach leverages a data-based model of the system, incorporating an empirical transfer function estimate to capture its behaviour.

Furthermore, in the state-of-the-art the impedance-matching theory is leveraged to synthesise controller, in panchromatic conditions, according to wave-related characteristic frequencies. Therefore, this study propose an insight, developing a framework to highlight the importance of defining a proper interpolating frequency.

To test the proposed methodology, a simple case study is conducted, illustrating the step-by-step process involved in achieving a power assessment. The results demonstrate the practical applicability of the outlined procedure and highlight the substantial impact of the mooring system on the overall system dynamics. By accounting for the mooring system's influence, the control synthesis and resulting power output are significantly influenced, emphasising the need for an accurate representation of the mooring system in performance assessments. Finally, it is important to emphasise that despite the simplicity of the proposed case study, the

selection of an inappropriate interpolating frequency in irregular conditions can lead to a significant decrease in power output.

We finish by noting that, it is crucial to recognise that the outlined case study lacks a realistic mechanism for energy production. In contrast, wave energy systems with more complex and intricate energy production mechanisms, such as PeWEC [30] or ISWEC [31], just to name a few, can exhibit resonant frequencies that differ from the device's resonant frequency. In such cases, the use of a carefully selected interpolating frequency becomes even more essential in defining a representative control action.

References

[1] J. Davidson and J. V. Ringwood, "Mathematical modelling of mooring systems for wave energy converters - a review," *Energies*, vol. 10, 2017.

[2] B. Paduano, E. Pasta, G. Papini, F. Carapellese, and G. Bracco, "Mooring influence on the productivity of a pitching wave energy converter," 2021, pp. 1–6.

[3] F. Niosi, L. Parrinello, B. Paduano, E. Pasta, F. Carapellese, and G. Bracco, "On the influence of mooring in wave energy converters productivity: the pewec case," 2021, pp. 1–6.

[4] F. Depalo, S. Wang, S. Xu, and C. G. Soares, "Design and analysis of a mooring system for a wave energy converter," *Journal of Marine Science and Engineering*, vol. 9, 7 2021.

[5] Y. Mao, T. Wang, and M. Duan, "A dnn-based approach to predict dynamic mooring tensions for semi-submersible platform under a mooring line failure condition," *Ocean Engineering*, vol. 266, p. 112767, 12 2022.

[6] H. Wei, L. Xiao, M. Liu, and Y. Kou, "Data-driven model and key features based on supervised learning for truncation design of mooring and riser system," *Ocean Engineering*, vol. 224, p. 108743, 3 2021.

[7] F. Cerveira, N. Fonseca, and R. Pascoal, "Mooring system influence on the efficiency of wave energy converters," *International Journal of Marine Energy*, vol. 3-4, pp. 65–81, 12 2013.

[8] J. Fitzgerald and L. Bergdahl, "Including moorings in the assessment of a generic offshore wave energy converter: A frequency domain approach," *Marine Structures*, vol. 21, pp. 23–46, 2008.

[9] E. Gubesch, N. Abdussamie, I. Penesis, and C. Chin, "Effects of mooring configurations on the hydrodynamic performance of a floating offshore oscillating water column wave energy converter," *Renewable and Sustainable Energy Reviews*, vol. 166, p. 112643, 9 2022.

[10] N. Faedo, E. Pasta, F. Carapellese, V. Orlando, D. Pizzirusso, D. Basile, and S. A. Sirigu, "Energy-maximising experimental control synthesis via impedance-matching for a multi degree-of-freedom wave energy converter," *IFAC-PapersOnLine*, vol. 55, pp. 345–350, 2022, 14th IFAC Conference on Control Applications in Marine Systems, Robotics, and Vehicles CAMS 2022.

[11] B. Tagliaferro, I. Martínez-Estévez, J. M. Domínguez, A. J. C. Crespo, M. Göteman, J. Engström, and M. Gómez-Gesteira, "A numerical study of a taut-moored point-absorber wave energy converter with a linear power take-off system under extreme wave conditions," *Applied Energy*, vol. 311, p. 118629, 2022.

[12] B. Robertson, H. Bailey, and B. Buckham, "Resource assessment parameterization impact on wave energy converter power production and mooring loads," *Applied Energy*, vol. 244, pp. 1–15, 2019.

[13] F. Carapellese, E. Pasta, B. Paduano, N. Faedo, and G. Mattiazzo, "Intuitive lti energy-maximising control for multi-degree of freedom wave energy converters: the pewec case," *Ocean Engineering*, 2022.

[14] B. Paduano, F. Carapellese, E. Pasta, S. Sergej, N. Faedo, and G. Mattiazzo, "Data-based control synthesis and performance assessment for moored wave energy conversion systems: the pewec case," *IEEE Transaction on sustainable energy (Accepted)*, 2023.

[15] N. Faedo, F. Carapellese, E. Pasta, and G. Mattiazzo, "On the principle of impedance-matching for underactuated wave energy harvesting systems," *Applied Ocean Research*, vol. 118, p. 102958, 1 2022.

[16] B. Paduano, F. Carapellese, E. Pasta, N. Faedo, and G. Mattiazzo, "Optimal controller tuning for a nonlinear moored wave energy converter via non-parametric frequency-domain techniques," 2022.

[17] M. Bonfanti and G. Giorgi, "Improving computational efficiency in wec design: Spectral-domain modelling in techno-economic optimization," *Journal of Marine Science and Engineering*, vol. 10, 2022, export Date: 12 June 2023; Cited By: 3.

[18] M. Bonfanti and S. A. Sirigu, "Spectral-domain modelling of a non-linear wave energy converter: Analytical derivation and computational experiments," *Mechanical Systems and Signal Processing*, vol. 198, 2023, export Date: 12 June 2023; Cited By: 0.

[19] J. M. J. Journee and W. W. Massie, *Offshore Hydromechanics*, 1st ed. Delft University of Technology, 2001.

[20] W. E. Cummins, "The impulse response function and ship motions," *Schiffstechnik*, vol. 9 (Heft 47, pp. 101–109, 1962.

[21] Orcina, "Orcaflex - documentation, 10.1b edition," 2020.

[22] T. L. Floyd and E. Pownell, *Principles of electric circuits*. PEARSON INDIA, 2000.

[23] ITTC, "Recommended procedures and guidelines 7.5-02-01-01: Guide to the expression of uncertainty in experimental hydrodynamics," 2014.

[24] J. Davidson, S. Giorgi, and J. V. Ringwood, "Linear parametric hydrodynamic models for ocean wave energy converters identified from numerical wave tank experiments," *Ocean Engineering*, vol. 103, pp. 31–39, 2015.

[25] R. Pintelon and J. Schoukens, *System Identification: A Frequency Domain Approach*. Wiley, 2004.

[26] J. Schoukens, R. Pintelon, E. V. D. Ouderaa, and J. Renneboog, "Survey of excitation signals for fft based signal analyzers," *IEEE Transactions on Instrumentation and Measurement*, vol. 37, pp. 342–352, 1988.

[27] R. Pintelon and J. Schoukens, *System Identification: A Frequency Domain Approach, Second Edition*, 2012, cited by: 996. [Online]. Available: https://www.scopus.com/inward/record.uri?eid=2-s2.0-84891585276&doi=10.1002%2f9781118287422&partnerID=40&md5=c4ed2cc5a43112831897b48a659c66e3

[28] M. Bonfanti, S. A. Sirigu, G. Giorgi, P. Dafnakis, G. Bracco, and G. Mattiazzo, "A passive control strategy applied to the iswec device: Numerical modelling and experimental tests," *International Journal of Mechanics and Control*, vol. 21, pp. 143–154, 2020, export Date: 12 June 2023; Cited By: 8.

[29] WMO, *Guide to Wave Analysis and Forecasting*, 1998, vol. 1998.

[30] F. Niosi, E. Begovic, C. Bertorello, B. Rinauro, G. Sannino, M. Bonfanti, and S. A. Sirigu, "Experimental validation of orcaflex-based numerical models for the pewec device," *Ocean Engineering*, vol. 281, p. 114963, 2023.

[31] S. A. Sirigu, G. Vissio, G. Bracco, E. Giorcelli, B. Passione, M. Raffero, and G. Mattiazzo, "Iswec design tool," *International Journal of Marine Energy*, vol. 15, pp. 201–213, 2016.